Eur. Phys. J. D (2018) 72: 178
https://doi.org/10.1140/epjd/e2018-90383-4

THE EUROPEAN PHYSICAL JOURNAL D

Regular Article

Can nonclassical correlations survive in the presence of asymmetric lossy channels?*

Alessia Allevi[1,2,a] and Maria Bondani[2]

[1] Department of Science and High Technology, University of Insubria, Via Valleggio 11, 22100 Como, Italy
[2] Institute for Photonics and Nanotechnologies, CNR, Via Valleggio 11, 22100 Como, Italy

Received 30 July 2018 / Received in final form 23 August 2018
Published online 11 October 2018

Abstract. Nonclassical correlations are a fundamental resource for applications involving multipartite systems. To assess nonclassicality, several different criteria can be applied to measured data. Here we compare three inequalities by applying them to a multi-mode twin-beam state, in which one of the two parties is transmitted through a varying lossy channel. We demonstrate, both theoretically and experimentally, that the asymmetry introduced by losses affects the three criteria in different ways, thus offering a tool for quantum optics applications.

1 Introduction

Since the pioneering work in which Hanbury-Brown and Twiss [1] discovered photon bunching in light emitted by a chaotic source, correlation functions [2] have been routinely used to experimentally investigate the nature of quantum states of light [3–5] at any intensity level. Formally, correlations are defined as normally ordered functions [6], even if in many experimental cases it is more convenient to express them in terms of measurable quantities by taking into account the model of the detection process.

From the experimental point of view, photon-number correlations are particularly useful to stress the statistical properties of light, beyond the direct reconstruction of photon-number distributions. For instance, in the mesoscopic photon-number domain, we have proved that the evaluation of photon-number correlations between the fields at the two outputs of a beam splitter is useful to better discriminate the statistical properties of light, such as to distinguish a superthermal statistics from a thermal one [7,8]. Moreover, photon-number correlations represent a powerful characterization tool in the case of bipartite or multipartite systems. Indeed, their existence is the main resource for several applications in the fields of quantum optics and quantum information, such as for the implementation of imaging protocols [9–12] and for the generation of sub-Poissonian states of light by conditioning measurements [13–16].

Since some applications require nonclassically correlated states, several nonclassicality criteria have been proposed [17–24] and experimentally tested over the years [25–29]. However, not all of them are easily applicable to experimental data [30–32], especially in the case of multipartite systems that can exhibit correlations of different nature among the different parties [13,33]. Moreover, some criteria are more robust than others, some are stricter and some others are weaker [34,35]. Quite recently, we have compared three of them, namely the Schwarz inequality, the noise reduction factor and a new inequality based on high-order correlation functions in the mesoscopic intensity domain [36]. In that work, we have shown that, in the case of a multi-mode twin-beam (TWB) state, the three criteria are always valid at any value of the mean photon number measured in the two parties, and that the new inequality is useful in case of highly populated TWB states [37].

However, there could be experimental conditions in which some differences among the criteria can emerge, thus demonstrating that they are not always equivalent. In this paper we consider the three criteria in the case in which one of the arms of the TWB state is affected by a varying loss. Investigating such condition represents a fundamental step towards the practical implementation of communication protocols involving quantum states of light. We probe that the noise reduction factor and the high-order criterion are not satisfied for every loss value and in particular we show that the inequality based on high-order correlations is stricter than the others in revealing nonclassicality.

2 Theory

In order to test the nonclassical nature of correlations, we consider three sufficient criteria written in terms of measurable quantities.

* Contribution to the Topical Issue "Quantum Correlations", edited by Marco Genovese, Vahid Karimipour, Sergei Kulik, and Olivier Pfister.

[a] e-mail: alessia.allevi@uninsubria.it

First of all, we introduce the noise reduction factor for detected photons, which is defined as

$$R = \sigma^2(m_1 - m_2)/\langle m_1 + m_2\rangle. \quad (1)$$

In equation (1), the subscripts 1 and 2 refer to the two parties, σ^2 is the variance of the difference between the photons measured in the two TWB arms, whereas the term $\langle m_1 + m_2\rangle$ is the shot-noise level. It has been shown that, whenever the value of R lies between $1-\eta$ and 1, the detected state is nonclassical since the fluctuations in the detected photon-number correlations are below the shot-noise level [25]. In the case of a perfectly generated multi-mode TWB state, R can be expressed as [38]

$$R = 1 - \frac{2\sqrt{\eta_1\eta_2}\sqrt{\langle m_1\rangle\langle m_2\rangle}}{\langle m_1\rangle + \langle m_2\rangle} + \frac{(\langle m_1\rangle - \langle m_2\rangle)^2}{\mu(\langle m_1\rangle + \langle m_2\rangle)}, \quad (2)$$

in which $\langle m_i\rangle$ (with $i = 1, 2$) is the mean number of photons generated in the i-arm, μ is the number of modes, whereas η_1 and η_2 are the quantum efficiencies in the two arms. In order to deal with the case of a varying lossy channel, we set $\langle m_1\rangle = \eta_1\langle n\rangle \equiv \eta\langle n\rangle = \langle m\rangle$ and $\langle m_2\rangle = \eta_2\langle n\rangle = \eta(1-\lambda)\langle n\rangle$, i.e. we assume that the detection chains have the same efficiency, and that the second channel is affected by an additional amount of loss with respect to the first channel, hereafter indicated as $\lambda = 1 - \eta_2/\eta_1$, where $\eta_2 \leq \eta_1$. Hence, equation (2) reduces to

$$R = 1 - \frac{2\eta(1-\lambda)}{2-\lambda} + \frac{\lambda^2}{(2-\lambda)}\frac{\langle m\rangle}{\mu}. \quad (3)$$

Note that for $\langle m\rangle/\mu \ll 1$, equation (3) reduces to $R = 1 - [2\eta(1-\lambda)]/(2-\lambda)$ and does not depend on the mean photon number.

The second sufficient nonclassicality criterion we consider is given by the Schwarz inequality [20], $S > 1$, written for detected photons, where

$$S = \frac{\langle m_1 m_2\rangle}{\sqrt{(\langle m_1^2\rangle - \langle m_1\rangle)\,(\langle m_2^2\rangle - \langle m_2\rangle)}}. \quad (4)$$

For a multi-mode TWB state, equation (4) can be rewritten in terms of measurable quantities as follows:

$$S = 1 + \frac{\mu}{\mu+1}\frac{\sqrt{\eta_1\eta_2}}{\sqrt{\langle m_1\rangle\langle m_2\rangle}}. \quad (5)$$

From this representation, it is clear that the Schwarz inequality is sensitive to the mean photon numbers and that it is particularly useful to test nonclassicality of low-photon-number states. Indeed, in that case the second term on the right-hand side of equation (5) becomes large. By setting again $\langle m_1\rangle = \eta_1\langle n\rangle \equiv \eta\langle n\rangle = \langle m\rangle$ and $\langle m_2\rangle = \eta_2\langle n\rangle = \eta(1-\lambda)\langle n\rangle$, equation (5) reduces to

$$S = 1 + \frac{\mu}{\mu+1}\frac{\eta}{\langle m\rangle}. \quad (6)$$

The quantity S in equation (6) testifies to the nonclassicality of TWB for each choice of η different from 0. Both R and S involve only first- and second-order correlation functions. Quite recently, we have shown that in some cases it is more useful to consider higher-order correlation functions, since they can highlight the correlated nature of the quantum states under study [39,40]. In particular, we have introduced a quantity involving correlation functions up to the fourth order, which, in the case of asymmetric losses, reads

$$B = \langle m\rangle^2(1-\lambda)\frac{g^{22} - [g^{13}]_s}{g^{11}} + \langle m\rangle\sqrt{(1-\lambda)}\frac{[g^{12}]_s}{g^{11}}, \quad (7)$$

where $g^{jk} = \langle m_1^j m_2^k\rangle(\langle m_1\rangle^j\langle m_2\rangle^k)^{-1}$ is the $(j+k)$th-order correlation function and $[g^{jk}]_s = (g^{jk} + g^{kj})/2$ represents its symmetrized version. If $B > 1$, the state is nonclassical. The high-order inequality is sensitive to the mean number of photons, like the Schwarz inequality. Different from it, this last criterion better emphasizes nonclassicality for high mean photon numbers. By applying the same assumption on the detection efficiencies used above, the high-order correlation functions g^{jk} read as follows:

$$\begin{aligned}
g^{11} &= G_\mu^1 + \frac{\eta}{\langle m\rangle}, \quad (8)\\
g^{21} &= G_\mu^2 + G_\mu^1\frac{1+2\eta}{\langle m\rangle} + \frac{\eta}{\langle m\rangle^2},\\
g^{12} &= G_\mu^2 + G_\mu^1\frac{1+2\eta(1-\lambda)}{(1-\lambda)\langle m\rangle} + \frac{\eta}{(1-\lambda)\langle m\rangle^2},\\
g^{22} &= G_\mu^3 + G_\mu^2\left(\frac{1+2\eta}{\langle m\rangle} + \frac{1+2\eta(1-\lambda)}{(1-\lambda)\langle m\rangle}\right)\\
&\quad + G_\mu^1\frac{1+2\eta^2(1-\lambda)+2\eta+2\eta(1-\lambda)}{(1-\lambda)\langle m\rangle^2} + \frac{\eta}{(1-\lambda)\langle m\rangle^3},\\
g^{31} &= G_\mu^3 + 3G_\mu^2\frac{1+\eta}{\langle m\rangle} + G_\mu^1\frac{1+6\eta}{\langle m\rangle^2} + \frac{\eta}{\langle m\rangle^3},\\
g^{13} &= G_\mu^3 + 3G_\mu^2\frac{1+\eta(1-\lambda)}{(1-\lambda)\langle m\rangle} + G_\mu^1\frac{1+6\eta(1-\lambda)}{(1-\lambda)^2\langle m\rangle^2}\\
&\quad + \frac{\eta}{(1-\lambda)^2\langle m\rangle^3},
\end{aligned}$$

where $\langle m\rangle = \sqrt{\langle m_1\rangle\langle m_2\rangle}$ is the average number of detected photons and $G_\mu^k = \prod_{j=1}^k(j+\mu)/\mu$. The expression of B is quite complex to analyze. In Figure 1a we plot the quantity B as a function of $(1-\lambda)$ for different choices of $\langle m\rangle$, whereas in Figure 1b we show B as a function of $\langle m\rangle$ for different choices of $(1-\lambda)$. In both cases, we set $\mu = 50$ and $\eta = 0.14$, which represent reliable experimental values (see Section 3). According to Figure 1a, for any value of $\langle m\rangle$, there is a threshold that is a value of $(1-\lambda)$ above which the nonclassicality of the investigated TWB is testified by the high-order correlation criterion. On the contrary, according to Figure 1b there are values of $(1-\lambda)$ for which the condition $B > 1$ is never satisfied. This means that in the case of a large amount of loss, the

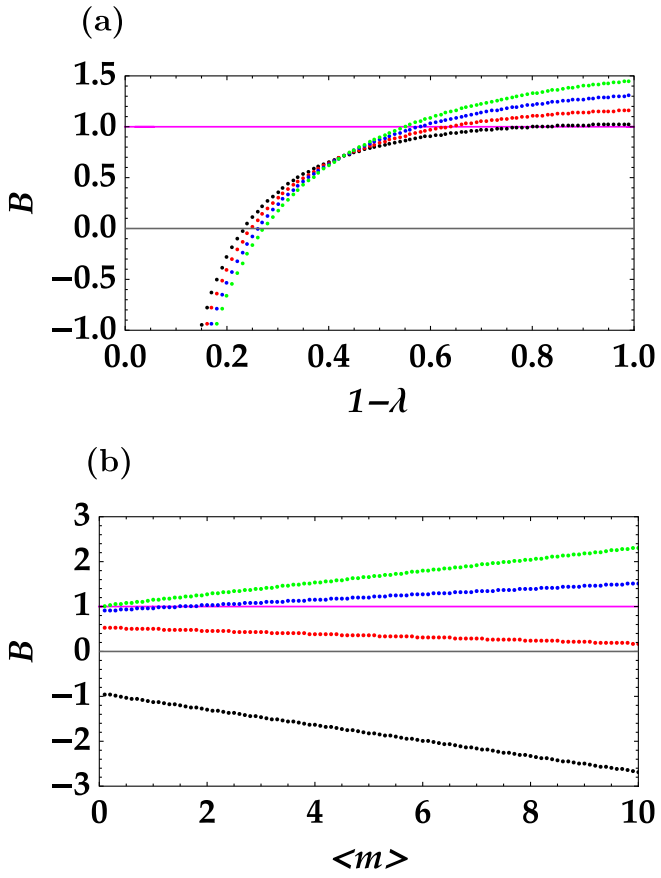

Fig. 1. (a) B as a function of $1-\lambda$ for different choices of $\langle m\rangle$ (black dots: $\langle m\rangle = 0.1$; red dots: $\langle m\rangle = 1$; blue dots: $\langle m\rangle = 2$; green dots: $\langle m\rangle = 3$). (b) B as a function of $\langle m\rangle$ for different choices of $1-\lambda$ (black dots: $1-\lambda = 0.15$; red dots: $1-\lambda = 0.35$; blue dots: $1-\lambda = 0.6$; green dots: $1-\lambda = 0.9$). In both cases $\mu = 50$ and $\eta = 0.14$. The magenta line at $B = 1$ represents the boundary condition.

nonclassical character of TWB cannot be revealed through this criterion anymore.

In order to better compare the three criteria presented above under realistic conditions, in the following section we present the experimental results obtained by considering a multi-mode TWB state in the mesoscopic intensity domain. A mesoscopic light state contains a sizeable number of photons (up to 100 photons), thus being more robust with respect to losses than a single-photon state.

3 Experiment

3.1 Experimental setup

The experimental setup is shown in Figure 2. The fundamental (F) and the third harmonic (TH) pulses of a mode-locked Nd:YLF laser regeneratively amplified at 500 Hz were sent to a type I β-Barium borate crystal (BBO_1, cut angle = 37°, 8-mm long) in order to produce the fourth harmonic (FH) at 262 nm. The FH beam was sent to a second type-I BBO crystal (BBO_2, cut angle = 46.7°, 6-mm long) to pump spontaneous parametric down-conversion and thus generate a multi-mode TWB state. Two twin portions at frequency degeneracy, i.e. at 523 nm, were then spectrally and spatially filtered and delivered to two hybrid photodetectors (HPDs, model R10467U-40, Hamamatsu Photonics) through two multi-mode fibers (600-μm core diamater). Each detector output was then amplified, synchronously integrated and digitized (ADC + PC). As already explained elsewhere [38,41], the detection process consists of two steps: photodetection by the photocathode and amplification. The first process is described by a Bernoullian convolution, whereas the second one can be well approximated by the multiplication of a constant gain factor. We have already demonstrated that the value of the gain can be obtained by means of a self-consistent method based on the very light to be measured [41]. Once the value of the gain is determined, we have direct access to the shot-by-shot number of detected photons and can thus evaluate the statistical properties of the measured states.

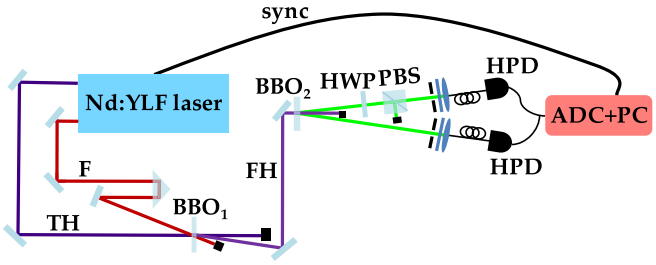

Fig. 2. Sketch of the experimental setup. See the text for details.

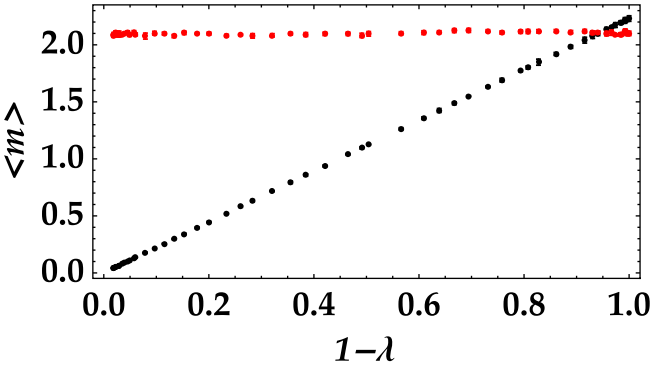

Fig. 3. Mean number of detected photons as a function of $1-\lambda$ in the two channels. The black dots + error bars (included in the size of the symbols) correspond to the lossy channel, and the red ones to the other arm.

In order to simulate a lossy channel, in one of the two arms we inserted a half-wave plate (HWP) followed by a polarizing cube beam splitter (PBS). We changed the amount of loss by rotating the HWP by 50° in steps of 2°. For each angle, 100,000 acquisitions were performed.

3.2 Experimental results

In Figure 3, we show the mean number of detected photons in both arms: in the lossy arm, the mean value, $\langle m_1\rangle$, changes according to the movement of the HWP.

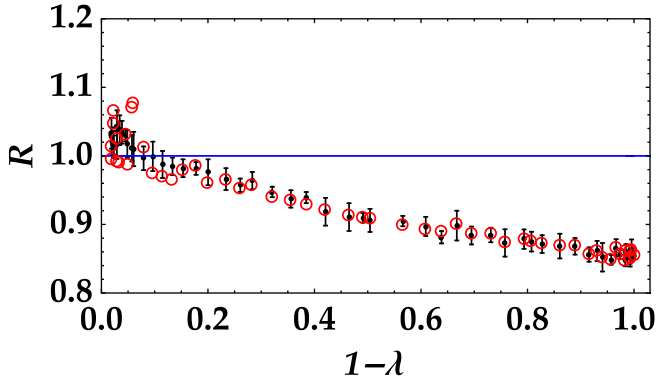

Fig. 4. Noise reduction factor as a function of $1-\lambda$. Black dots + error bars: data; red circles: theoretical expectation according to equation (3). The blue line at $R=1$ represents the boundary condition.

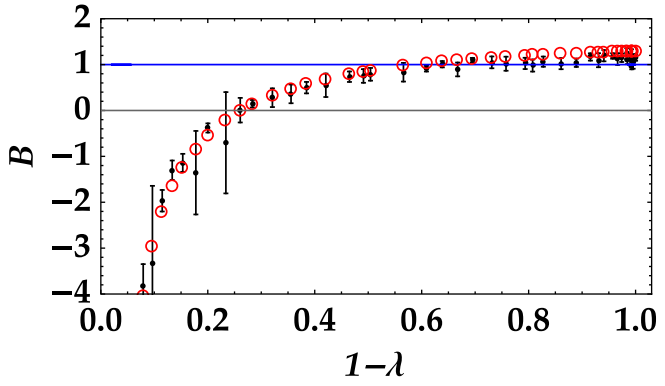

Fig. 6. B parameter as a function of $1-\lambda$. Black dots + error bars: data; red circles: theoretical expectation according to equation (7). The blue line at $B=1$ represents the boundary condition.

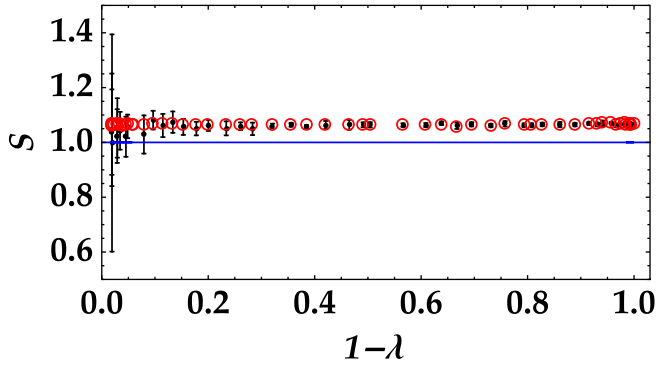

Fig. 5. Schwarz parameter as a function of $1-\lambda$. Black dots + error bars: data; red circles: theoretical expectation according to equation (6). The blue line at $S=1$ represents the boundary condition.

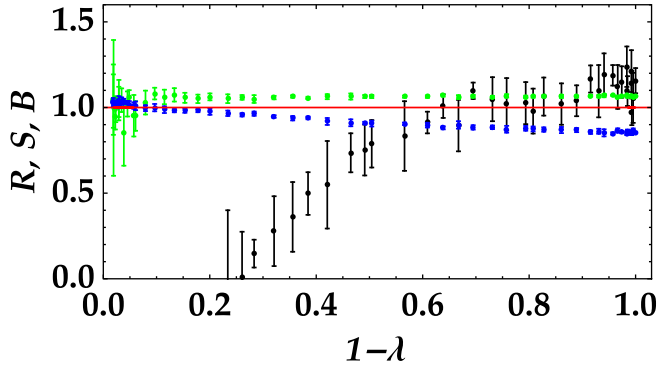

Fig. 7. Noise reduction factor (blue dots), S parameter (green dots) and B parameter (black dots) as functions of $1-\lambda$. The red line at $R=1$ represents the boundary condition.

On the contrary, the mean value $\langle m_2\rangle$ in the other arm is constant. In order to investigate if the nonclassical correlations exhibited by the TWB can survive asymmetric losses in the two arms, we consider the three inequalities introduced in Section 2. In Figure 4 we plot the noise reduction factor as a function of $1-\lambda$, which represents the fraction of photons surviving losses. The data are shown as black dots, whereas the theoretical values calculated according to equation (3) are shown as red circles. In particular, we used the measured values of $\langle m_1\rangle$ and $\langle m_2\rangle$. The number of modes μ was estimated by the first two moments of photon-number statistics, whereas η was obtained from the experimental values of the noise reduction factor setting $R=1-\eta$ [15]. Finally, the quantity $1-\lambda$ was determined as the ratio between the current value of $\langle m_1\rangle$ and its maximum value. We note that in Figure 4 for small mean numbers of photons, the noise reduction factor becomes larger than 1. Indeed, for such values $R>1$, since the third term on the right-hand side of equation (3) becomes not negligible for every very small unbalancing.

On the contrary, Figure 5 shows that, as expected from equation (6), the Schwarz inequality is always satisfied, no matter the mean value and the amount of loss λ in only one arm. In the figure, the experimental data are shown as black dots, whereas the theoretical expectations, shown as red circles, were obtained by calculating equation (6) in the experimental values of $\langle m_1\rangle$, $\langle m_2\rangle$, μ, and η.

Finally, in Figure 6 we plot the high-order inequality as a function of $(1-\lambda)$. In this case, the presence of a threshold in the experimental data is clearly evident, as already demonstrated by the theoretical expectations of Figure 1a. The value of $1-\lambda$ at which B becomes larger than 1 is not only different from the value at which $R>1$, but also larger, thus emphasizing that the high-order inequality is a more demanding criterion than the noise reduction factor.

In order to better remark this point, in Figure 7, we compare the three criteria by showing only the experimental data for the sake of clarity. We note that for the present system, the three criteria exhibit different behaviors. In particular, the presence of an asymmetric amount of loss in the two twin arms can prevent or not the observation of nonclassicality depending on the chosen criterion. It is not surprising that the high-order inequality is much more sensitive to losses than the other two considered in this work since it involves correlations up to the fourth order. On the contrary, the Schwarz inequality, which is connected only to the first-order correlation, is satisfied

for each value of $1-\lambda$. These results testify that while in the presence of equal amounts of losses in the two arms the three criteria are always satisfied [38], in the case of asymmetric losses a hierachy among the inequalities emerges. Moreover, from Figure 7 we notice that the high-order inequality amplifies the presence of asymmetric losses even if when they are small.

The different performance of the nonclassicality criteria in the presence of asymmetric losses suggests that the three inequalities can be exploited in different ways. For instance, the Schwarz inequality reveals the very quantum nature of TWB for each choice of asymmetric loss. This means that such criterion cannot be used to highlight the presence of a disturbance in the transmission of the light signal. On the contrary, the noise reduction factor and the high-order inequality are sensitive to the different amounts of loss in the twin arms and thus they can be used to certify the availability of a good-quality TWB state for applications like quantum imaging protocols. Indeed, the noise-reduction-based criterion is exploited for sub-shot-noise imaging [42], whereas the high-order inequality can be used in high-order correlation imaging [40,43].

4 Conclusions

In this paper, we explored the applications of three different nonclassicality criteria based on photon-number correlations in the case of a multi-mode TWB state, in which the two parties were affected by different amounts of loss. Indeed, such an investigation is of fundamental importance to understand at which extent the existence of quantum correlations is preserved in asymmetric lossy channels. We demonstrated, both theoretically and experimentally, that the Schwarz inequality is always satisfied, whereas the noise reduction factor and the high-order correlation criterion exhibit a threshold, i.e. a value of loss above which it is not possible to reveal the presence of nonclassical photon-number correlations. We note that the threshold is different for the two criteria, being lower for the inequality involving correlation functions up to the fourth order. The investigated situation emphasizes the hierarchy among the different inequalities, which is connected to the fact that the higher the order of correlation involved, the more critical the nonclassicality criterion.

Author contribution statement

Both the authors conceived the experimental scheme. A.A. carried out the experiment and processed the experimental data. Both the authors contributed to the interpretation of the results and were involved in the preparation of the manuscript. Both the authors have read and approved the final manuscript.

References

1. R. Hanbury-Brown, R.Q. Twiss, Nature (London) **177**, 27 (1956)
2. E. Wolf, L. Mandel, *Optical Coherence and Quantum Optics* (Cambridge University Press, Cambridge, UK, 1995)
3. M. Blazek, W. Elsäßer, Phys. Rev. A **84**, 063840 (2011)
4. G. Harder, T.J. Bartley, A.E. Lita, S.W. Nam, T. Gerrits, C. Silberhorn, Phys. Rev. Lett. **116**, 143601 (2016)
5. A. Allevi, M. Bondani, Sci. Rep. **7**, 16787 (2017)
6. R. Glauber, Phys. Rev. **130**, 2529 (1963)
7. A. Allevi, M. Bondani, Opt. Lett. **40**, 3089 (2015)
8. A. Allevi, S. Cassina, M. Bondani, Quantum Meas. Quantum Metrol. **4**, 26 (2017)
9. F. Ferri, D. Magatti, A. Gatti, M. Bache, E. Brambilla, L.A. Lugiato, Phys. Rev. Lett. **94**, 183602 (2005)
10. N. Samantaray, I. Ruo-Berchera, A. Meda, M. Genovese, Light Sci. Appl. **6**, e17005 (2017)
11. A. Meda, E. Losero, N. Samantaray, F. Scafirimuto, S. Pradyumna, A. Avella, I. Ruo-Berchera, M. Genovese, J. Opt. **19**, 094002 (2017)
12. M. Genovese, J. Opt. **18**, 073002 (2016)
13. A. Ferraro, M.G.A. Paris, M. Bondani, A. Allevi, E. Puddu, A. Andreoni, J. Opt. Soc. Am. B **21**, 1241 (2004)
14. A. Ourjoumtsev, R. Tualle-Brouri, P. Grangier, Phys. Rev. Lett. **96**, 213601 (2006)
15. M. Lamperti, A. Allevi, M. Bondani, R. Machulka, V. Michálek, O. Haderka, J. Peřina, Jr., J. Opt. Soc. Am. B **31**, 20 (2014)
16. T.Sh. Iskhakov, V.C. Usenko, U.L. Andersen, R. Filip, M.V. Chekhova, G. Leuchs, Opt. Lett. **41**, 2149 (2016)
17. R. Short, L. Mandel, Phys. Rev. Lett. **51**, 384 (1983)
18. D.N. Klyshko, Phys. Usp. **39**, 573 (1996)
19. T. Richter, W. Vogel, Phys. Rev. Lett. **89**, 283601 (2002)
20. W. Vogel, D.G. Welsch, *Quantum Optics* (John Wiley & Sons, Inc., New York, 2006)
21. W. Vogel, Phys. Rev. Lett. **100**, 013605 (2008)
22. A. Miranowicz, M. Bartkowiak, X. Wang, Y.X. Liu, F. Nori, Phys. Rev. A **82**, 013824 (2010)
23. S. Olivares, M.G.A. Paris, Int. J. Mod. Phys. B **27**, 1345024 (2013)
24. I.I. Arkhipov, J. Peřina, Jr., J. Peřina, A. Miranowicz, Phys. Rev. A **91**, 033837 (2015)
25. M. Bondani, A. Allevi, G. Zambra, M.G.A. Paris, A. Andreoni, Phys. Rev. A **76**, 013833 (2007)
26. I.N. Agafonov, M.V. Chekhova, G. Leuchs, Phys. Rev. A **82**, 011801 (2010)
27. M. Avenhaus, K. Laiho, M.V. Chekhova, C. Silberhorn, Phys. Rev. Lett. **104**, 063602 (2010)
28. T.J. Bartley, G. Donati, X.-M. Jin, A. Datta, M. Barbieri, I.A. Walmsley Phys. Rev. Lett. **110**, 173602 (2013)
29. J. Peřina, Jr., I.I. Arkhipov, V. Michálek, O. Haderka, Phys. Rev. A **96**, 043845 (2017)
30. P. Horodecki, Phys. Lett. A **232**, 333 (1997)
31. R. Simon, Phys. Rev. Lett. **84**, 2726 (2000)
32. I.I. Arkhipov, J. Peřina, Jr., J. Svozilík, A. Miranowicz, Sci. Rep. **6**, 26523 (2016)
33. I.I. Arkhipov, J. Peřina, Jr., O. Haderka, A. Allevi, M. Bondani, Sci. Rep. **6**, 33802 (2016)
34. I.P. Degiovanni, M. Bondani, E. Puddu, A. Andreoni, M.G.A. Paris, Phys. Rev. A **76**, 062609 (2007)
35. I.P. Degiovanni, M. Genovese, V. Schettini, M. Bondani, A. Andreoni, M.G.A. Paris, Phys. Rev. A **79**, 063836 (2009)
36. A. Allevi, S. Olivares, M. Bondani, Phys. Rev. A **85**, 063835 (2012)

37. A. Allevi, M. Lamperti, M. Bondani, J. Peřina, Jr., V. Michálek, O. Haderka, R. Machulka, Phys. Rev. A **88**, 063807 (2013)
38. A. Allevi, M. Bondani, Adv. At. Mol. Opt. Phys. **66**, 49 (2017)
39. T. Iskhakov, A. Allevi, D.A. Kalashnikov, V.G. Sala, M. Takeuchi, M. Bondani, M. Chekhova, Eur. Phys. J. Special Topics **199**, 127 (2011)
40. M. Bondani, A. Allevi, A. Andreoni, Eur. Phys. J. Special Topics **203**, 151 (2012)
41. M. Bondani, A. Allevi, A. Agliati, A. Andreoni, J. Mod. Opt. **56**, 226 (2009)
42. G. Brida, M. Genovese, I. Ruo Berchera, Nat. Photon. **4**, 227 (2010)
43. K. Chan, M. O′Sullivan, R. Boyd, Opt. Lett. **34**, 3343 (2009)